# Formation of Planetary Systems through population synthesis and N-body simulations

M.P. Ronco[1,2,3]

[1] *Instituto de Astrofísica, Pontificia Universidad Católica de Chile, Núcleo Milenio de Formación Planetaria, Chile*
[2] *Instituto de Astrofísica de La Plata, CONICET–UNLP, Argentina*
[3] *Facultad de Ciencias Astronómicas y Geofísicas, UNLP, Argentina*

*Contact* / mronco@astro.puc.cl

**Resumen** / En este documento describimos brevemente los resultados más importantes de los trabajos de investigación realizados durante mi doctorado. Este proyecto estuvo dedicado a estudiar la formación y evolución de diferentes tipos de sistemas planetarios tanto durante la etapa gaseosa de formación, que involucra los primeros millones de años de vida de un sistema planetario, como durante la era post-gas en la cual priman las interacciones gravitatorias entre los proto-planetas y planetesimales que se formaron al final de la primera etapa. Enfocamos nuestro análisis en la formación de planetas rocosos en las regiones internas del disco, particularmente en la zona de habitabilidad, prestando especial atención a los procesos y fuentes de acreción de agua durante toda la evolución de los sistemas. El mayor desafío del proyecto fue estudiar la formación de sistemas planetarios similares al nuestro con el objetivo de obtener un mejor entendimiento sobre cómo pudo haberse formado el Sistema solar, combinando diferentes etapas de la formación planetaria.

**Abstract** / In this manuscript we briefly describe the main results of the research works developed during my PhD. This project was dedicated to study the formation and evolution of different kinds of planetary systems, both during the gaseous formation stage, which involves the first million years of life of a planetary system, and during the post-gas stage, where the gravitational interactions between the proto-planets and planetesimals formed at the end of the first stage play a key role. We focused our analysis on the formation of rocky planets in the inner regions of the disk, particularly within the habitable zone, paying special attention to the water accretion processes and sources throughout the whole evolution of the planetary systems. The main challenge of this project was to analyze the formation of systems similar to our own with the aim of having a better understanding on how the Solar system could had formed combining different stages of planet formation.

*Keywords* / planets and satellites: dynamical evolution and stability — planets and satellites: formation — methods: numerical

## 1. Introduction

Since the discovery of the first extrasolar planet orbiting a solar-type star (Mayor & Queloz, 1995), the study of planetary formation, which until then had been limited only to our Solar system, had a significant growth. Up to March 2019, and with the increase in the quantity and quality of the different missions, 3997 exoplanets of great variety have been discovered orbiting nearby stars (`http://exoplanet.eu/` Schneider et al., 2011). Much of these planets form part of more than 650 multiple planet systems, and in many cases, the central star of these systems is similar to our Sun. However, we have not yet been able to find a Solar System Analog (SSA): a planetary system formed simultaneously by rocky planets in the inner regions of the disk and by at least a gas giant planet similar to Saturn or Jupiter in the outer zones of the disk.

These multiple planetary systems represent the final snapshot of different complex processes and stages of planet formation and have triggered theoretical studies about the formation and evolution of different kinds of planetary systems.

For the last ten years different models of planet formation have been developed to study the first stages of the formation of planetary systems when the protoplanetary disk still presents a gaseous component. Population synthesis works, like the pioneer works of Ida & Lin (2004a,b, 2008), have been performed with the aim to reproduce the mass vs. semimajor-axis diagrams of the current sample of exoplanets, and to better understand the main processes of planetary formation (see Benz et al., 2014, for a detailed review and references therein).

On the other hand, several works have studied the formation of terrestrial planets in the post-oligarchic growth regime, via purely N-body calculations, in different dynamical scenarios or within the framework of the formation of our Solar system (Raymond et al., 2004, 2009; O'Brien et al., 2006; Ronco & de Elía, 2014). However, the initial embryo and planetesimal distributions adopted to analyze the late accretion stage of planet formation are typically selected arbitrarily without linking them with previous evolutionary stages.

Raymond et al. (2004, 2006) studied the formation

of terrestrial planets around solar-type stars affected by the perturbational effects of a Jovian planet located in the outer regions of the disk. Then, Mandell et al. (2007) explored the same scenario but including a migrating gas giant planet, and later Fogg & Nelson (2009) showed that this phenomenon does not prevent rocky planet formation in the inner regions. More recently Zain et al. (2018) considered different dynamical environments around solar-type stars, harboring different kinds of planets as the main perturbers of the systems, with the aim of analyzing the rocky planet formation and water delivery within the habitable zone. They found that the formation of water-rich planets in the habitable zone seems to be a common process in all the studied scenarios.

The original goal of this project was to analyse the formation of different kinds of planetary systems during the post-gas phase through the development of pure N-body simulations. However, we were aware that, in order to get more reliable results, we had to link different stages of planetary formation to avoid starting our post-gas phase simulations from arbitrary initial conditions. To do that we improved our model of planet formation including some of the most relevant physical phenomena that take place in the formation of a planetary system during the gaseous phase, and we then performed a planetary population synthesis to determine the main properties of the disks that lead to the formation of SSA. The last stage of this project consisted in the development of N-body simulations of SSA starting from the planetary and planetesimal distributions that resulted at the end of the gaseous phase. During this part of the work we analyzed the formation of rocky planets within the habitable zone and their final water contents. Here we summarize the main results and conclusions of this PhD Thesis, but for the readers interest, the complete manuscript can be found in the Repositorio Institucional de la UNLP* (Spanish version).

## 2. Results

The first stages of this work were dedicated to study the formation of rocky worlds in planetary systems without gaseous giant planets. Previous observational (Cumming et al., 2008) and theoretical works (Mordasini et al., 2009; Miguel et al., 2011) had suggested that this kind of planetary systems would be common in the Universe. Following these results we first developed N-body simulations to analyze the late accretion stage of rocky planet formation (Ronco & de Elía, 2014) considering arbitrary initial conditions, i.e. arbitrary planetesimal and embryo distributions. Later, we improved this study using a planet formation code (Guilera et al., 2010) able to compute the formation of a planetary system during the gaseous phase and adopted the results of this stage as initial conditions for the late accretion stage N-body simulations (Ronco et al., 2015). The main conclusion of this last work was that, although the final outcomes of our simulations of planet formation were globally similar both using arbitrary or more realistic initial conditions, the use of initial conditions obtained from a model of planet formation resulted in different accretion histories for each of the final rocky planets of our simulations, particularly for those that remained within the habitable zone. Therefore, they presented different characteristics in terms of their final masses and final water contents which could significantly change the resulting planetary systems.

### 2.1. Population synthesis of planetary systems

Motivated by these results we improved our model of planet formation (Guilera et al., 2010, 2011, 2014), which we now call PLANETALP, and we applied it to the study of the formation and evolution of SSA with the aim of getting better initial conditions to then study the long term evolution of this kind of systems. Following our definition, an SSA is a planetary system that presents rocky planets in the inner region of the disk and presents at least one gas giant planet, like Jupiter or Saturn, beyond the current Mars location, that is, beyond 1.5 au.

The 1D planet formation code PLANETALP describes the time evolution of a planetary system during the gaseous phase and incorporates important physical phenomena for the formation of planetary systems. The model presents a protoplanetary disk characterized by two components: a gaseous disk that evolves in time due to an $\alpha$-viscosity driven accretion (Pringle, 1981; Shakura & Sunyaev, 1973) and due to EUV photoevaporation by the central star (Dullemond et al., 2007; D'Angelo & Marzari, 2012), and a solid component represented by a planetesimal population that suffers accretion, scattering (Alibert et al., 2005) and ejection by the embryos (Ida & Lin, 2004a), and radial drift due to the gas drag. Moreover, PLANETALP takes into account the evolution of the eccentricities and inclinations of the planetesimals affected by embryo gravitational excitations (Ohtsuki et al., 2002) and by the damping due to the nebular gas drag (Rafikov, 2004; Chambers, 2008).

The gaseous component, characterized by a gas surface density, is given by

$$\Sigma_{\rm g}(R) = \Sigma_{\rm g}^0 \left(\frac{R}{R_{\rm c}}\right)^{-\gamma} e^{-\left(\frac{R}{R_{\rm c}}\right)^{2-\gamma}}, \quad (1)$$

where $R$ is the radial coordinate in the midplane of the disk, $R_{\rm c}$ is a characteristic radius of the disk, $\gamma$ is the exponent that represents the surface density gradient and $\Sigma_{\rm g}^0$ is a normalization constant. The planetesimal surface density profile is given by

$$\Sigma_{\rm p}(R) = \Sigma_{\rm p}^0 \eta_{\rm ice} \left(\frac{R}{R_{\rm c}}\right)^{-\gamma} e^{-\left(\frac{R}{R_{\rm c}}\right)^{2-\gamma}}, \quad (2)$$

where $\Sigma_{\rm p}^0 \sim 0.01\Sigma_{\rm g}^0$, and $\eta_{\rm ice}$ is a function that represents an increase in the amount of solid material due to the condensation of water beyond the iceline; this represents the location in the disk beyond which water condensates, at $\sim 2.7$ au (Hayashi, 1981).

In addition, the model presents an embryo population which grows by accretion of planetesimals (Inaba et al., 2001), gas, and due to their fusion taking into account their atmospheres (Inamdar & Schlichting,

*http://sedici.unlp.edu.ar/handle/10915/66476

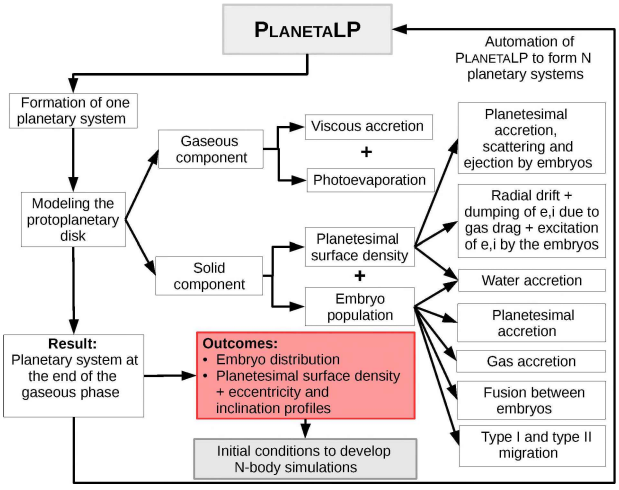


Figure 1: Diagram showing the operation of PLANETALP. The details of the implementation of each physical process can be found in Ronco et al. (2017)

.

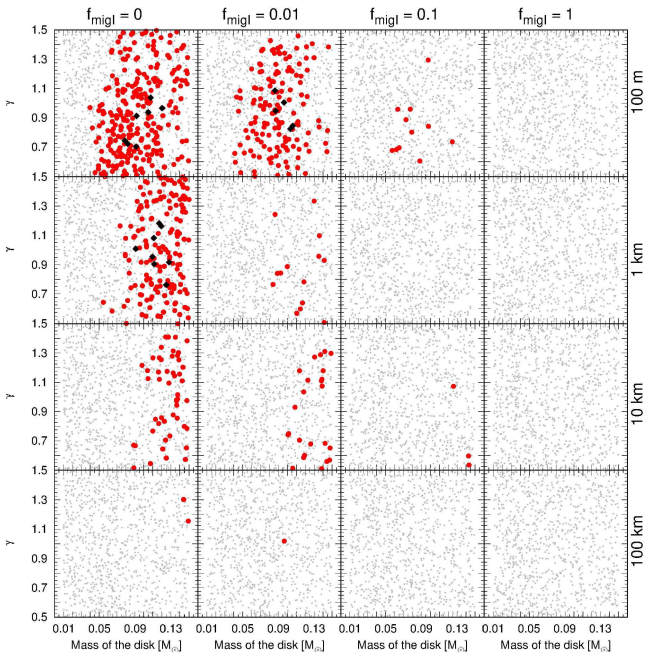


Figure 2: Results of the population synthesis developed with PLANETALP. Each block corresponds to a particular formation scenario with different type I migration rates and different planetesimal sizes, and each point represents a set of disk parameters for a particular planetary system in the $M_{\rm d} - \gamma$ plane. The red points represent sets of disk parameters that formed SSA at the end of the gaseous stage. Grey points represent the rest of the systems that are not SSA. Particularly, the black diamonds are SSAs that present all their disk parameters between $\pm\sigma$, simultaneously.

2015). When these planets are not massive enough to open a gap in the gaseous disk they suffer type I migration, which in idealized vertically isothermal disks like the ones we considered, always produces fast and inward migration rates (Tanaka et al., 2002). When the planets are massive enough to open a clear gap in the gas surface density (Crida et al., 2006) they suffer type II migration (Armitage, 2007). Both, planetesimal and embryo populations, also incorporate a water radial distribution. The initial percentage per unit mass of water in embryos and planetesimals is 0% inside the iceline and a percentage that can randomly vary between 10% and 66% beyond the iceline.

Fig. 1 summarizes the operation of the code. The details of the implementation of all these phenomena can be found in Ronco et al. (2017) and in previous versions of this code (Guilera et al., 2010, 2011, 2014).

With the aim of determining which are the most suitable formation scenarios and disk parameters of SSA, we automated PLANETALP to perform thousands of simulations and to do a population synthesis analysis. It is important to remark that the main goal of this population synthesis, unlike previous works of similar kind (Ida & Lin, 2004a; Mordasini et al., 2009; Alibert et al., 2013), was not to reproduce the mass vs. semimajor-axis diagram of the current exoplanet population, but to see what kind of planetary systems can be formed without following any observable distribution in the disk parameters. Thus, the disk parameters, such as the mass $M_{\rm d}$ and the characteristic radius $R_{\rm c}$ of the disk, the $\gamma$ exponent of the density profile and the $\alpha$-viscosity parameter among others, were randomly selected from uniform distributions and for which the values of the ranges were extracted mainly from previous observational works (Andrews et al., 2009, 2010). It is also important to remark that the selected disk parameters for each protoplanetary disk were combined in such a way that the gas disk always dissipated in timescales ranging from 1 to 12 Myr, in agreement with observational works (Pfalzner et al., 2014).

Fig. 2 shows the results of the population synthesis. Each square block represents a different formation scenario with different type I migration rates and different planetesimal sizes. As type I migration can be very fast, following Miguel et al. (2011) we introduced a reduction factor $f_{\rm migI}$ which considers possible mechanisms that can cancel or reduce the planet inward migration 10 and 100 times. The size of the planetesimals is still uncertain within the standard model of core accretion. Thus, as in Fortier et al. (2013), we considered single sizes of planetesimals of 100 m, 1 km, 10 km and 100 km per simulation. Each point in each block represents a planetary system formed from a particular set of disk parameters. The red points represent those systems that became SSA at the end of the gaseous phase. The small grey points represent all the other kinds of formed planetary systems (see Sec. 4.1 in Ronco et al., 2017, for more details). We developed 1000 simulations per each block, representing a total of 16000 simulations, but the SSA only represented a 4.3% of all of them, and the most suitable formation scenarios to get them were those formed from small planetesimals and with low/null type I migration rates. However, we found SSA throughout the whole range of disk parameters except for disk masses smaller than $0.04 M_{\odot}$. Therefore, SSA could only form in relatively massive disks.

An important finding to highlight, that serendipi-

tously arose during the analysis of the population synthesis (Ronco et al., 2017), was that a very small percentage of the total of the performed simulations, indeed only 6 from the total of 16000, presented a gas giant planet in an extended orbit at the end of the gaseous phase, beyond 40 au and up to 100 au. A detailed analysis of these results showed us that these planets were migrating outwards in synchrony with the outer boundary of the gas surface density gap opened by the photoevaporation process. This finding naturally explains the possible formation of gas giant planets in stable wide orbits and was latter studied in detail by Guilera et al. (2017) who computed the vertical structure of the disk and included type I migration rates for non-isothermal disks (Paardekooper et al., 2010, 2011).

Fig. 3 shows an example of the time evolution of one of the modeled planetary systems that ended up being an SSA once the gas disk had dissipated. Panel a) shows the time evolution, represented by the color scale, of the gaseous component as a function of the distance to the central star due to viscous accretion and photoevaporation. Panel b) shows the planetesimal surface density evolution due to radial drift, ejection, scattering and accretion by the embryos. Finally panel c) shows the time evolution of an embryo population distributed between 0.1 au and 30 au in a mass vs. semimajor-axis plane. The embryos grow by accreting gas and planetesimals, and via mergers between them. This planetary system formed from planetesimals of 1 km and in an scenario without type I migration. The disk parameters are $M_{\rm d} = 0.13 M_{\odot}$, $\gamma = 0.9$, $R_{\rm c} = 34$ au, $\alpha = 1.1 \times 10^{-3}$, and the dissipation timescale is $\tau = 6.65$ Myr.

Finally, Fig. 4 shows the configurations of ten different SSA formed from different planetesimal sizes and with different type I migration rates. These planetary configurations present the planet distribution (colored points) and the remnant of the planetesimal surface density after the gas completely dissipated (black curve) which would later be used as initial conditions to analyze the late accretion stage of planet formation. The big black and grey points represent Jupiter-like planets and Saturn analogs, respectively, while the colored points with black borders are Neptune-like planets. The rest of the colored points represent planetary embryos with different masses and different fractions of water by mass. As it can be seen, none of the formed embryos of the inner regions are water-rich at the end of this stage.

## 2.2. Long term evolution of SSA

The main goal of this part of the project was to analyze the long term evolution of SSAs once the gas had dissipated, through the development of N-body simulations. We focused primarily on the formation of rocky planets and their water contents in the inner regions of the disk, particularly within the habitable zone (HZ) (see Sec. 5.1 in Ronco & de Elía, 2018, for details about the considered limits of this region). We then made use of the results of the population synthesis as the initial conditions for our N-body simulations. Thus, the planetesimal remnant and embryo distributions at the end of the gas stage were our starting points to study the late accretion stage of SSA formation.

As we mentioned in the previous section, SSAs represent only a 4.3% of all the population synthesis simulations, this is only 688 SSAs. However, and due to the high computational cost of the N-body simulations of this kind, it was not viable to develop simulations for all of them. We show in Fig. 4 the most representative SSA for each formation scenario that were chosen to be simulated.

To carry out our simulations we used the hybrid integrator of the MERCURY code which uses a symplectic algorithm for the treatment of the interaction between objects with separations greater than three Hill radii, and a Burlisch–Stoer method for close encounters(Chambers, 1999). This version of the code does not include planet or planetesimal fragmentation, thus, collisions between all the bodies were treated as inelastic mergers, which conserved mass and water contents. Due to the high numerical cost of the N-body simulations we only considered gravitational interactions between planets and between planets and planetesimals, but planetesimals were not self-interacting. The number of planetary embryos depend on the results of the previous formation stage but is in the range of 40 to 90. The available mass in planetesimals also depends on the results of planet formation model, however we always considered 1000 planetesimals per simulation with semimajor-axis selected using an acceptance–rejection method that follows their surface density profile. Planetary embryos and planetesimals present physical densities of 3 gr cm$^{-3}$ and 1.5 gr cm$^{-3}$, respectively.

We integrated each simulation for 200 Myr assuming that the rocky planets in our Solar system may have formed within this timescale (Touboul et al., 2007; Jacobson et al., 2014) and we considered a 6 day timestep to compute the inner orbit with enough precision. The energy conservation in our simulations was better than one part in $10^3$. Embryos and gas giant planets were considered in circular and coplanar orbits. However the orbital eccentricities and inclinations for the planetesimal population were results of the gas-phase evolution. The rest of the orbital parameters, such as the argument of pericentre $\omega$, the longitude of ascending node $\Omega$, and the mean anomaly M, were taken randomly between 0° and 360° for all the solid bodies. We performed at least 10 simulations for each of the formation scenarios of Fig. 4 since the accretion process is very stochastic.

We first analyzed the long term evolution of four reference scenarios, which are the planetary systems formed from planetesimals of 100 km, 10 km, 1 km, and 100 m and without suffering type I migration during the gaseous phase ($S_1$, $S_4$, $S_6$ and $S_9$ scenarios of Fig. 4). We then developed simulations for the rest of the planetary systems, affected by different type I migration rates, and studying how this phenomenon could change the previous results.

The detailed description of the dynamical evolution of each of the four reference scenarios is not included here but can be found in Sect. 5.2 of Ronco & de Elía (2018). Here we only highlight their most important differences and similarities focusing on the regions where

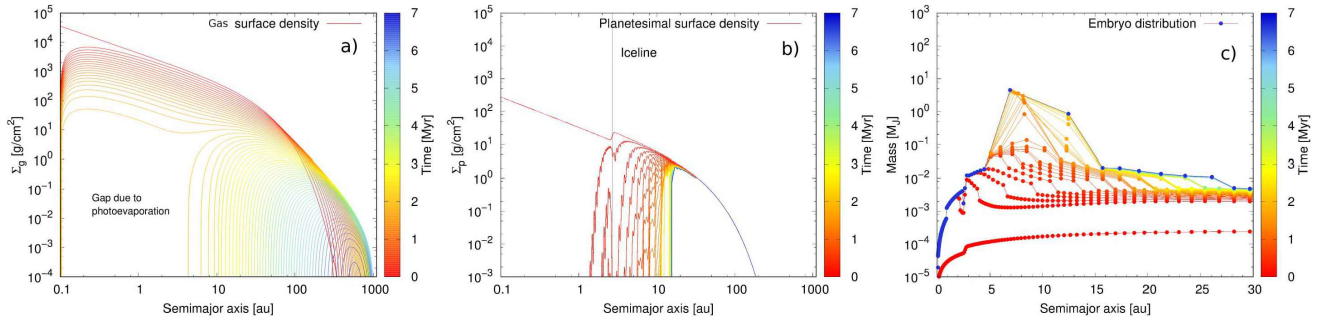


Figure 3: Example of the time evolution of the gas surface density (a), the planetesimal surface density (b) and the embryo distribution (c) of a planetary system similar to our own plotted every 0.1 Myr. The disk parameters for this system are: $M_{\rm d} = 0.13 M_{\odot}$, $\gamma = 0.92$, $R_{\rm c} = 34$ au, and $\alpha = 10^{-3}$. The dissipation timescale for this particular disk is $\tau = 6.65$ Myr.

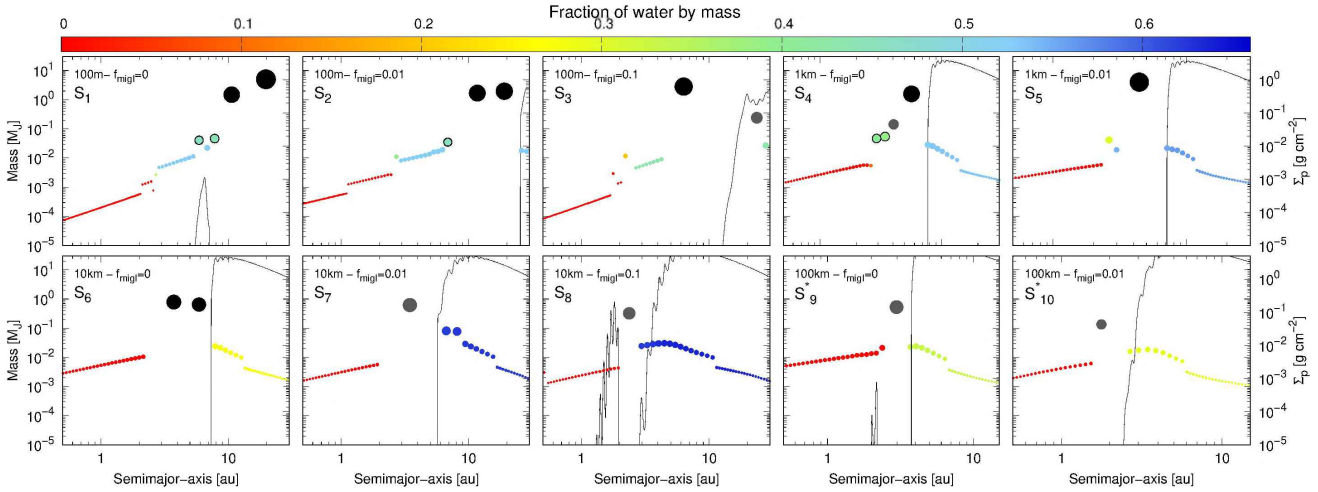


Figure 4: Ten SSA configurations at the end of the gaseous phase obtained with the population synthesis. Each panel shows a mass vs. semimajor-axis vs. planetesimal surface density plane for SSA formed in different formation scenarios. Each colored point represents a planetary embryo, the black and grey big points represent Jupiter and Saturn analogs, respectively, while the colored points with black borders are icy giants, like Neptune. The solid black line in all the planetary systems represents the remnant of planetesimal when the gas is completely dissipated. The colorscale represents the final amounts of water by mass in each planet and the size of each planet is represented in logarithmic-scale.

potentially habitable planets** (PHP) could form.

It can be seen from Fig. 4 that the mass of the gas giant planets of the different scenarios grows as the size of the planetesimals decreases. In those formation scenarios with low-mass gas giants, like $S_9$, the Saturn-like planet suffered a significant inward embryo-driven migration during the N-body simulations that located this planet at the outer edge of the HZ, preventing PHP from forming. Thus, formation scenarios formed from big planetesimals did not present any particular interest.

The general configuration at the end of the gaseous phase of those scenarios formed with planetesimals of 1 km, 10 km, and 100 km are quite different from the one formed with planetesimals of 100 m. By inspecting and comparing scenarios $S_1$, $S_4$, $S_6$ and $S_9$ of Fig. 4 it can be seen that the planetesimal population is located inside the giants positions in $S_1$, instead of outside, the gas giant planets are further away from the central star than in $_4$, $S_6$ and $S_9$, and a water-rich embryo population is directly next to the dry one, in the inner region of the disk. These differences conducted to different results in the final configurations of the N-body simulations.

The main similarities between all the formation scenarios were related to the mass remotion (embryos and planetesimals) mechanisms. Mass ejection from the systems was the most efficient remotion process, both for embryos and planetesimals, and to a lesser extent, accretion and collisions with the central star.

The configuration of the inner regions of all the scenarios was in general a quick process that occured within the first 1 Myr of evolution for scenarios of 100 km and 10 km, and within the first 10 Myr and 50 Myr for scenarios of 1 km and 100 m, respectively.

The analysis of the final planetary configurations showed us that the efficiency in the formation of PHPs seems to be higher for planetary systems formed from small planetesimals than from bigger ones, being completely null for planetesimals of 100 km. Fig. 5 shows three snapshots in time for an N-body simulation of

**Our definition of a potentially habitable planet (PHP) is that of a planet that remains within the limits of the HZ. A PHP will be of astrobiological interest if it is capable of harboring a water content superior to that estimated on Earth, which is $\sim 0.1\%$ by mass.

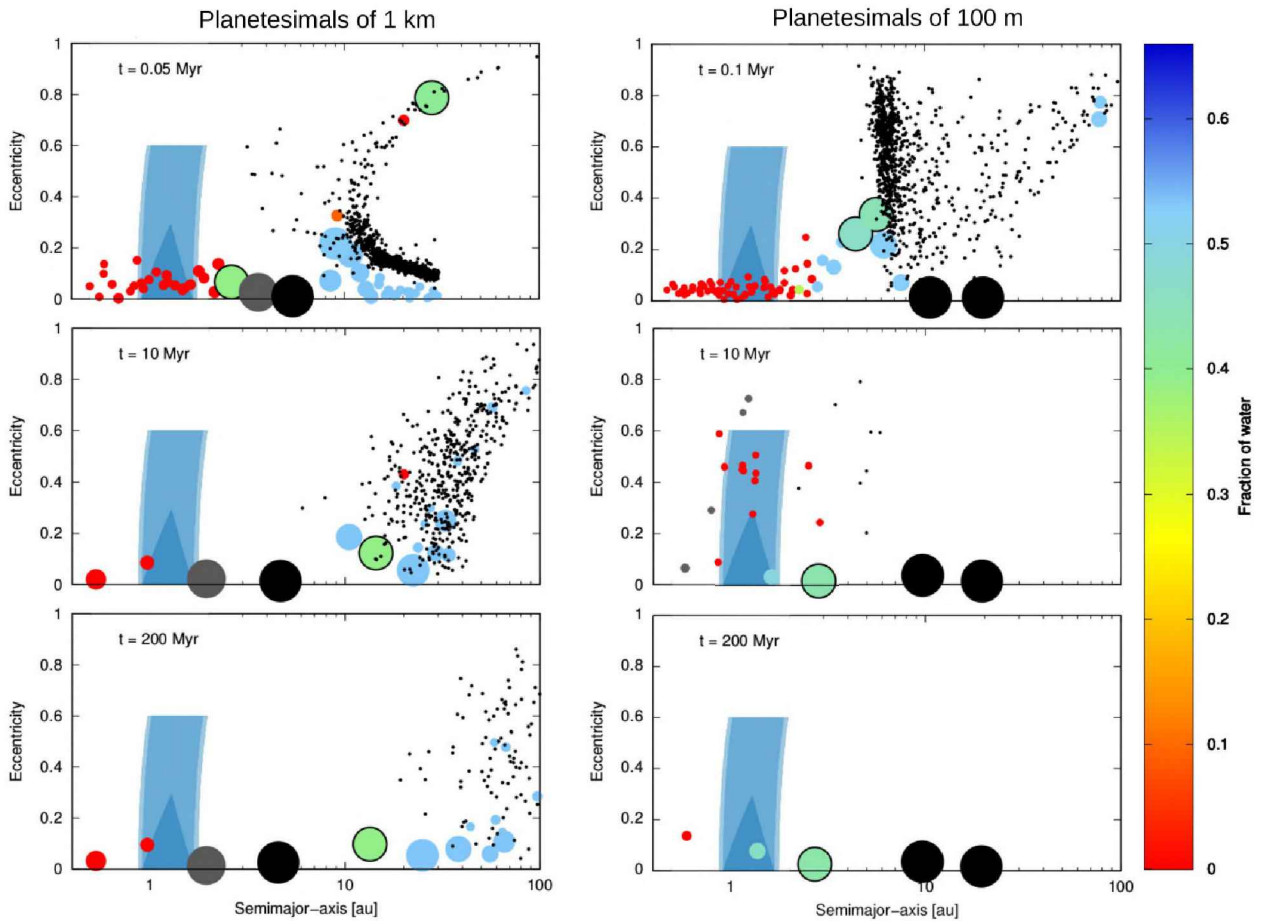


Figure 5: Time evolution of one of the ten developed simulations of planetary configuration $S_4$ (left) and $S_1$ (right) from Fig. 4. The shaded areas represent the HZ regions. Planets are plotted as coloured circles, planetesimals as black dots and the giant planets are represented in grey (Saturn-like planets) and black (Jupiter-like planets). The big coloured planets with black borders represent Neptune-like planets. The size of the planets is represented by a lineal relation between the mass and the size, where the size for the smallest embryo is the double of the size of the planetesimals. The giant planets do not follow this relation. The colorscale represents the fraction of water by mass.

scenario $S_4$ (left) formed from planetesimals of 1 km and for scenario $S_1$ (right) formed from planetesimals of 100 m. It can be seen how both scenarios formed PHP but with different characteristics. While the masses of those PHPs of $S_1$ were in the range of the Super-Earths ($2M_\oplus - 8M_\oplus$), the masses of the PHPs in the other scenarios were in the range of the Super and Mega-Earths ($8M_\oplus - 30M_\oplus$) . Besides, scenarios formed from planetesimals of 100 m were the only ones capable of forming PHPs of real interest that presented high water contents. And although considering the four reference scenarios the most common type of PHPs seemed to be the dry ones, since they were formed in three of four scenarios, considering all the developed simulations water-rich PHPs were the most abundant, representing more than 65% of the whole simulated PHP population. Finally, for the N-body simulations of planetary systems that were affected by type I migration rates during the gaseous phase, the general result was that this phenomenon seems to favour the formation of PHPs in planetary systems formed from small planetesimals, but avoids their formation in systems formed from big planetesimals.

The PHPs formed within our simulations were contrasted in mass, and radius, vs. semimajor-axis diagrams with the current discovered PHPs around Solar-type stars (PHLs Exoplanet Catalog of the Planetary Habitability Laboratory - `http://phl.upr.edu`). Fig. 6 shows that there is an overlap of both populations, the detected and the simulated ones. Although this is not a confident comparison since none of these observed PHPs are confirmed part of a planetary system similar to our own, we were able to form PHPs in regions of the diagrams that were already explored and where exoplanets were discovered.

## 3. Main Conclusions

We improved and automated our new planet formation code PlanetaLP, including several important physical phenomena for the planet formacion process, in order to perform a population synthesis analysis. The primary goal of this study was to find suitable formation scenarios and protoplanetary disk parameters for the for-

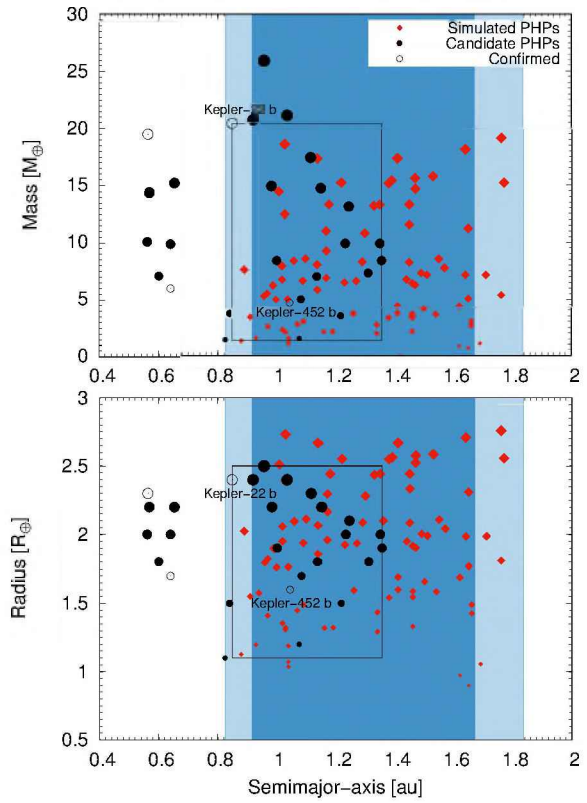


Figure 6: Mass (top) and radius (bottom) vs. semimajor-axis diagrams for the simulated PHPs (red diamonds) and the observed PHPs around solar-type stars (black points). The shaded areas represent the HZ and the black square delimits the region in where we find both, the observed and the simulated planetes. Kepler-452 b and Kepler-22 b are the only two confirmed exoplanets within this region.

mation of SSAs, this is, planetary systems with rocky planets in the inner region of the disk and at least a gas giant planet beyond 1.5 au. Then we used the final SSA planet and planetesimal configurations as initial conditions with the aim of studying the long term evolution of those systems with N-body simulations once the gas of the disk had dissipated.

The population synthesis analysis showed us that the formation of SSA is not common. In fact only 4.3% of the developed simulations resulted in planetary systems with this arquitecture. However we found SSA throughout the whole range of disk parameters considered, except in scenarios with disks less massive than $0.04M_{\odot}$. The configurations found in these systems were quite diverse. The most representative ones presented between 1 and 3 gaseous giant planets, like Jupiter or Saturn, between 0 and 4 icy giant planets, like Neptune, and between 100 and 200 rocky planets throughout the protoplanetary disk. Finally, the most favorable formation scenarios for SSA were those formed from small planetesimals, with sizes between 100 m and 1 km, and with low and null type I migration rates.

Using the results after the dissipation of the gas disk as starting point, we performed more than 200 N-body simulations to analyze the long term evolution of some of the SSA configurations obtained with the population synthesis. The main goal of this part of the work was to study how do rocky planets form in this kind of systems, and how many of them and with what percentages of water by mass remain within the habitable zone. The reference formation scenarios, formed from planetesimals of 100 m, 1 km, 10 km and 100 km without type I migration showed that the efficiency in the formation of PHP strongly depends on the size of the planetesimals from which they were formed. The SSA formed from small planetesimals were the most efficient ones in the formation of PHP, being completely null for the SSA formed from large planetesimals (100 km).

Another important result was that those SSA that suffered moderate type I migration rates during the gas stage of planet formation showed the same tendency: the efficiency in the formation of PHP is higher for those planetary systems formed from small planetesimals. Two kinds of PHP were formed during our simulations: dry and water-rich. By considering the four reference scenarios, the most common type of PHPs seem to be the dry ones since we formed them in three of four scenarios. However, considering the final number of PHPs formed within all the developed simulations, the result is just the other way around: water-rich are the most common ones since they represent most of the PHPs population (more than 65%).

*Acknowledgements:* I would first like to thank mi PhD Advisor, Dr. Gonzalo C. de Elía, for his support and guidance during these first years of investigation. I thank the Facultad de Ciencias Astronómicas y Geofísicas where I developed my PhD and also the Consejo Nacional de Investigaciones Científicas y Técnicas de la República Argentina (CONICET) who awarded me with a PhD fellowship. Finally, I would like to thank the Varsavsky Foundation and the Asociación Argentina de Astronomía for the "Carlos M. Varsavsky" award received during the last Second Binational Meeting, and the AAA for the economic assistance that facilitated my participation during the meeting.

## References

Alibert Y., et al., 2005, A&A, 434, 343
Alibert Y., et al., 2013, A&A, 558, A109
Andrews S.M., et al., 2009, ApJ, 700, 1502
Andrews S.M., et al., 2010, ApJ, 723, 1241
Armitage P.J., 2007, ApJ, 665, 1381
Benz W., et al., 2014, Protostars and Planets VI, 691–713
Chambers J., 2008, Icarus, 198, 256
Chambers J.E., 1999, MNRAS, 304, 793
Crida A., Morbidelli A., Masset F., 2006, Icarus, 181, 587
Cumming A., et al., 2008, PASP, 120, 531
D'Angelo G., Marzari F., 2012, ApJ, 757, 50
Dullemond C.P., et al., 2007, Protostars and Planets V, 555–572
Fogg M.J., Nelson R.P., 2009, A&A, 498, 575
Fortier A., et al., 2013, A&A, 549, A44
Guilera O.M., Brunini A., Benvenuto O.G., 2010, A&A, 521, A50
Guilera O.M., Miller Bertolami M.M., Ronco M.P., 2017, MNRAS, 471, L16
Guilera O.M., et al., 2011, A&A, 532, A142
Guilera O.M., et al., 2014, A&A, 565, A96
Hayashi C., 1981, Progress of Theoretical Physics Supplement, 70, 35
Ida S., Lin D.N.C., 2004a, ApJ, 604, 388

Ida S., Lin D.N.C., 2004b, ApJ, 616, 567
Ida S., Lin D.N.C., 2008, ApJ, 685, 584-595
Inaba S., et al., 2001, Icarus, 149, 235
Inamdar N.K., Schlichting H.E., 2015, MNRAS, 448, 1751
Jacobson S.A., et al., 2014, Nature, 508, 84
Mandell A.M., Raymond S.N., Sigurdsson S., 2007, ApJ, 660, 823
Mayor M., Queloz D., 1995, Nature, 378, 355
Miguel Y., Guilera O.M., Brunini A., 2011, MNRAS, 417, 314
Mordasini C., et al., 2009, A&A, 501, 1161
O'Brien D.P., Morbidelli A., Levison H.F., 2006, Icarus, 184, 39
Ohtsuki K., Stewart G.R., Ida S., 2002, Icarus, 155, 436
Paardekooper S.J., Baruteau C., Kley W., 2011, MNRAS, 410, 293
Paardekooper S.J., et al., 2010, MNRAS, 401, 1950
Pfalzner S., Steinhausen M., Menten K., 2014, ApJl, 793, L34
Pringle J.E., 1981, ARAA, 19, 137
Rafikov R.R., 2004, AJ, 128, 1348
Raymond S.N., Quinn T., Lunine J.I., 2004, Icarus, 168, 1
Raymond S.N., Quinn T., Lunine J.I., 2006, Icarus, 183, 265
Raymond S.N., et al., 2009, Icarus, 203, 644
Ronco M.P., de Elía G.C., 2014, A&A, 567, A54
Ronco M.P., de Elía G.C., 2018, MNRAS, 479, 5362
Ronco M.P., de Elía G.C., Guilera O.M., 2015, A&A, 584, A47
Ronco M.P., Guilera O.M., de Elía G.C., 2017, MNRAS, 471, 2753
Schneider J., et al., 2011, A&A, 532, A79
Shakura N.I., Sunyaev R.A., 1973, A&A, 24, 337
Tanaka H., Takeuchi T., Ward W.R., 2002, ApJ, 565, 1257
Touboul M., et al., 2007, Nature, 450, 1206
Zain P.S., et al., 2018, A&A, 609, A76